Supplementary Materials

Structure, DFT Calculations and Magnetic Characterization of Coordination Polymers of Bridged Dicyanamido-metal(II) Complexes

Franz A. Mautner [1*], Patricia Jantscher [1], Roland C. Fischer [2], Ana Torvisco [2], Ramon Vicente [3], Tolga N.V. Karsili [4], Salah S. Massoud [4*]

[1] Institut für Physikalische and Theoretische Chemie, Technische Universität Graz, A-8010 Graz, Austria

[2] Institut für Anorganische Chemie, Technische Universität Graz, A-8010 Graz, Austria

[3] Department de Química Inorgànica, Universitat de Barcelona, Martí i Franquès 1-11, 08028 Barcelona, Spain

[4] Department of Chemistry, University of Louisiana at Lafayette, P.O. Box 44370 Lafayette, LA 70504, USA

Table of Contents:

Table S1. The groud state minimum energy of Co(II) or Mn(II) centers of **1** and **2**, respectively in their high-spin and low-spin configurations.

Spin Multiplicity	**Absolute Energy / Hartree**
Co(II) – quartet (**1**)	-2975.5856
Co(II) - singlet	-2975.4610
Mn(II) – sextet (**2**)	-2893.3463
Mn(II) - singlet	-2893.2149

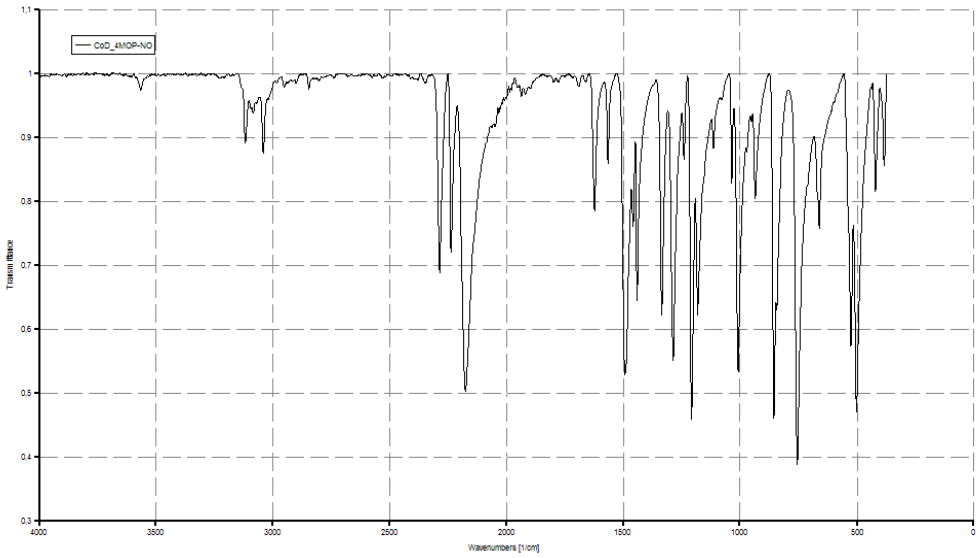

Figure S1. IR spectrum of *catena*-[Co($\mu_{1,5}$-dca)$_2$(4-MOP-NO)$_2$] (**1**)

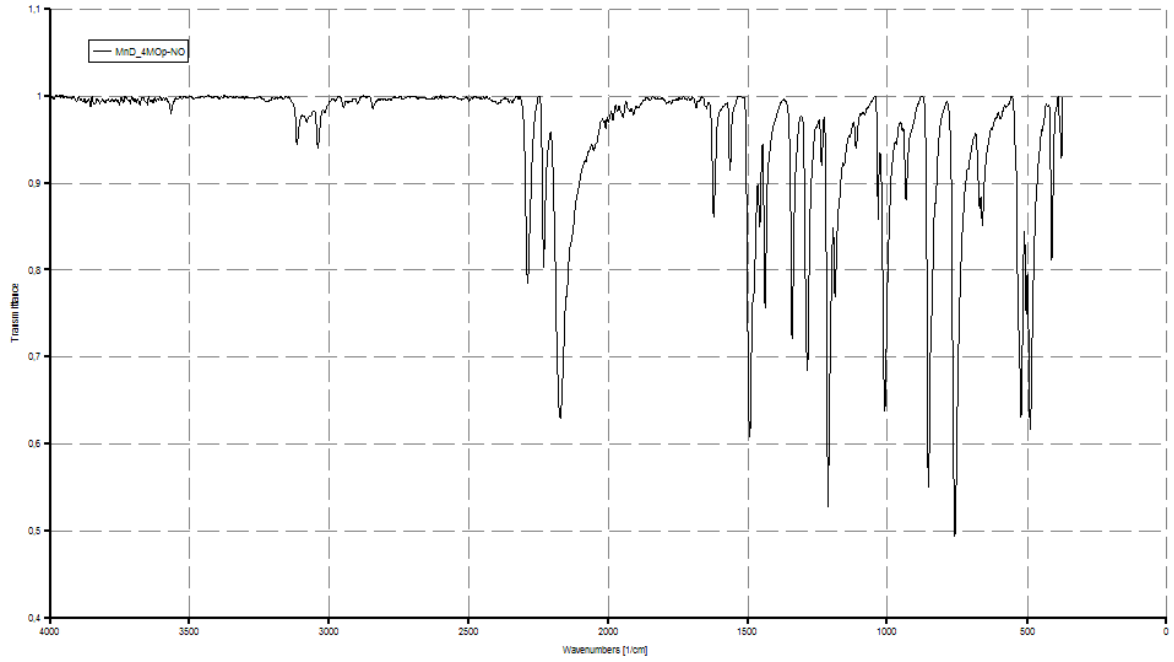

Figure S2. IR spectrum of *catena*-[Mn($\mu_{1,5}$-dca)$_2$(4-MOP-NO)$_2$] (**2**)

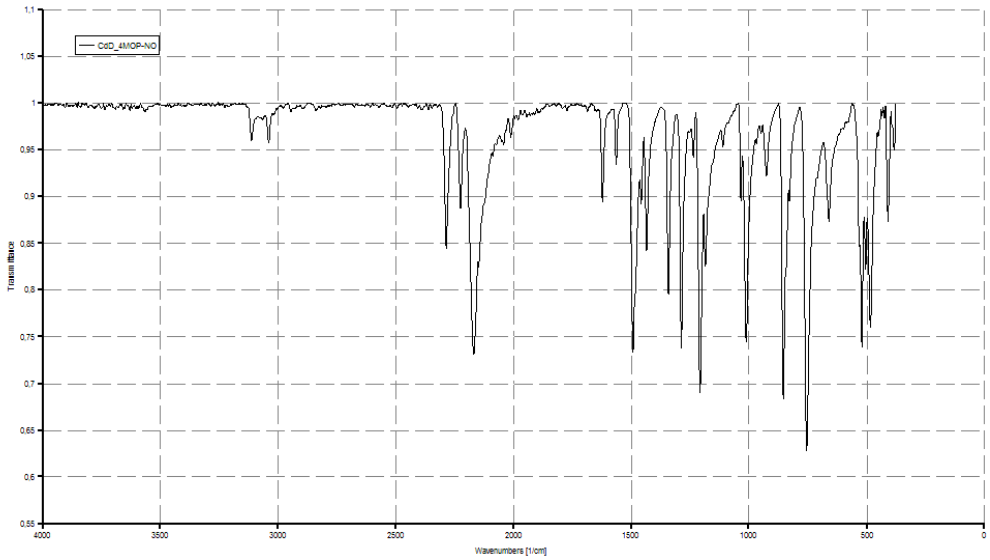

Figure S3. IR spectrum of *catena*-[Cd($\mu_{1,5}$-dca)$_2$(4-MOP-NO)$_2$] (**3**)

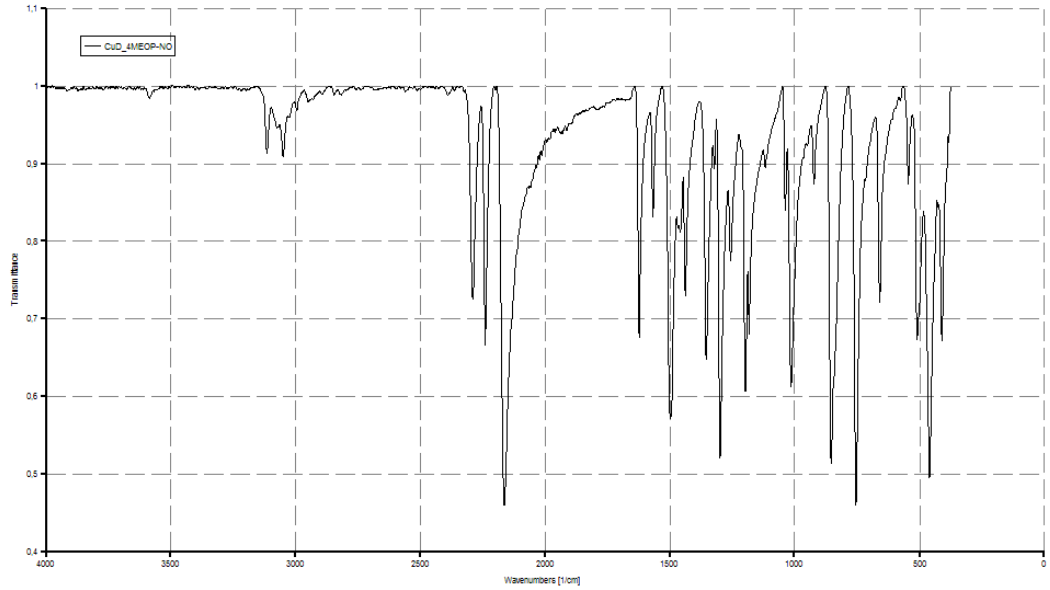

Figure S4. IR spectrum of [Cu(κ^1-dca)$_2$(4-MOP-NO)$_2$] (**4**)

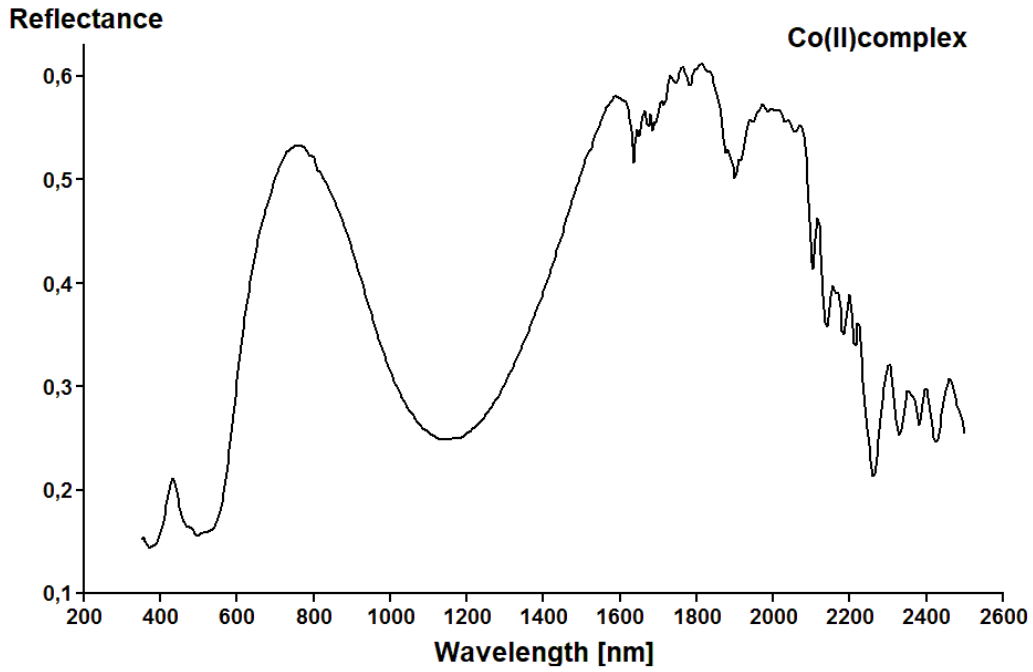

Figure S5. The solid state UV-VIS-NIR spectrum of *catena*-[Co($\mu_{1,5}$-dca)$_2$(4-MOP-NO)$_2$] (**1**)

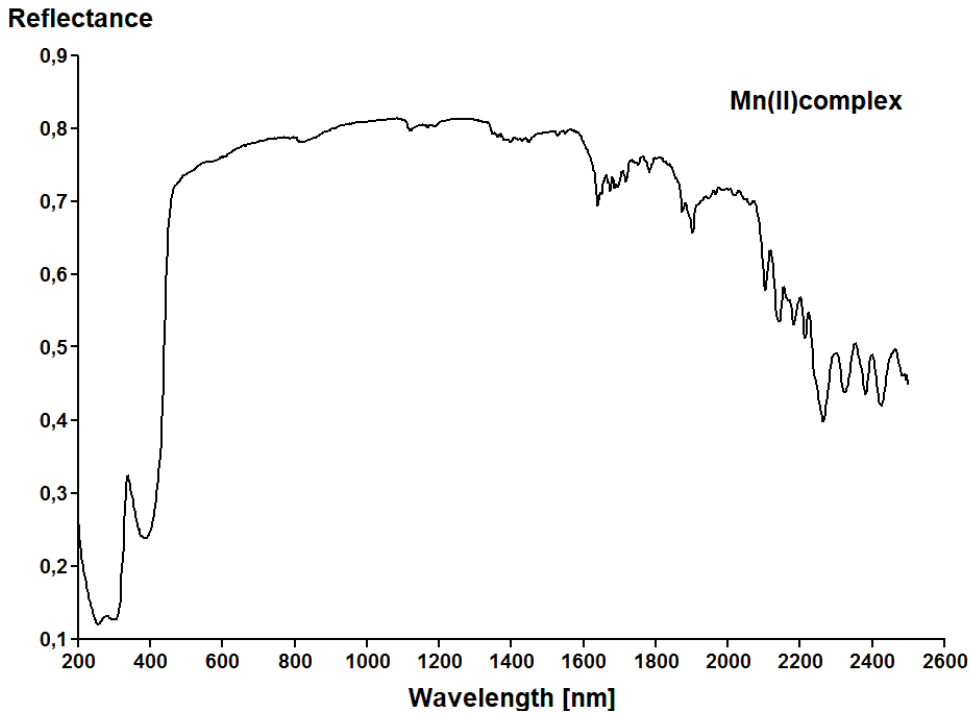

Figure S6. The solid state UV-VIS-NIR spectrum of *catena*-[Mn($\mu_{1,5}$-dca)$_2$(4-MOP-NO)$_2$] (**2**). (Uncorrected spectrum, offset at approx.810 nm is caused by detector change)

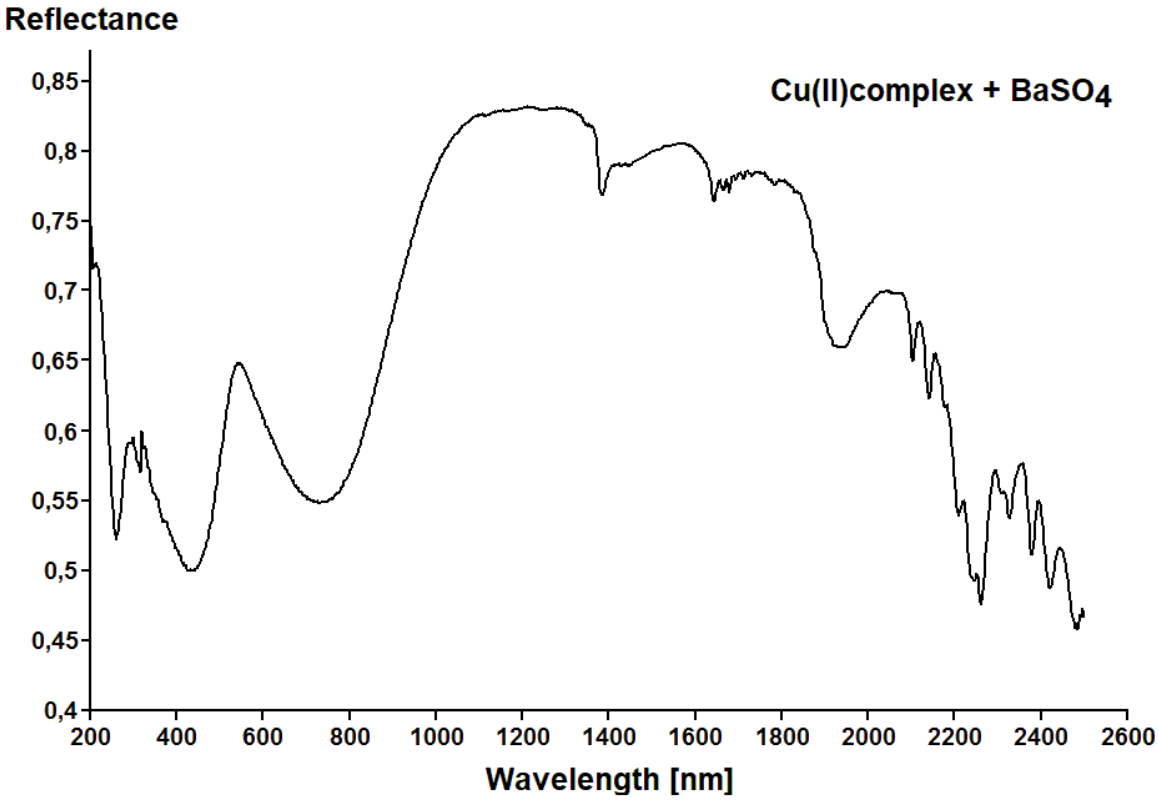

Figure S7. The solid state UV-VIS-NIR spectrum of mixture of $[Cu(\kappa^1\text{-dca})_2(4\text{-MOP-NO})_2]$ (**4**) with $BaSO_4$ (1:5 w:w) (uncorrected spectrum; the spike at approx. 315 nm is caused by change of UV lamp)

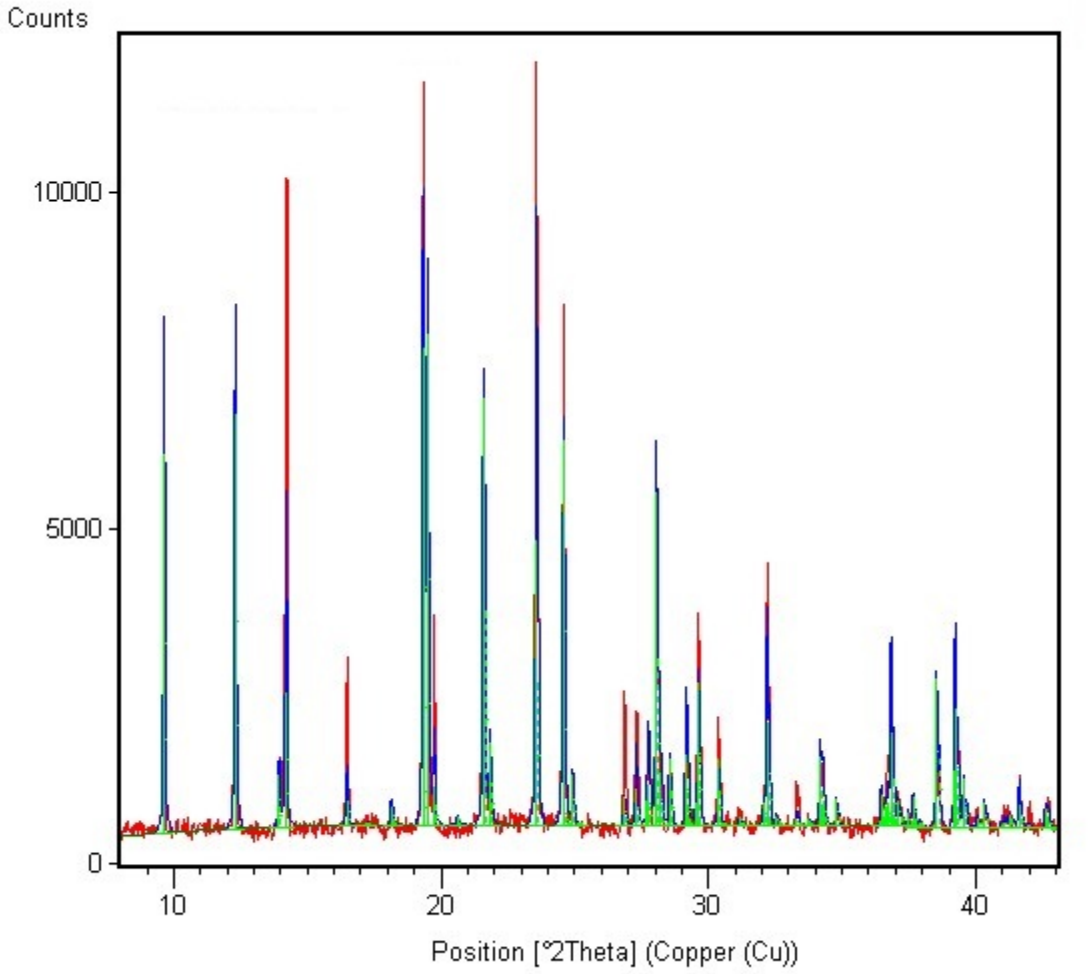

Figure S8. Observed and simulated X-ray powder pattern of *catena*-[Co($\mu_{1,5}$-dca)$_2$(4-MOP-NO)$_2$] (**1**)

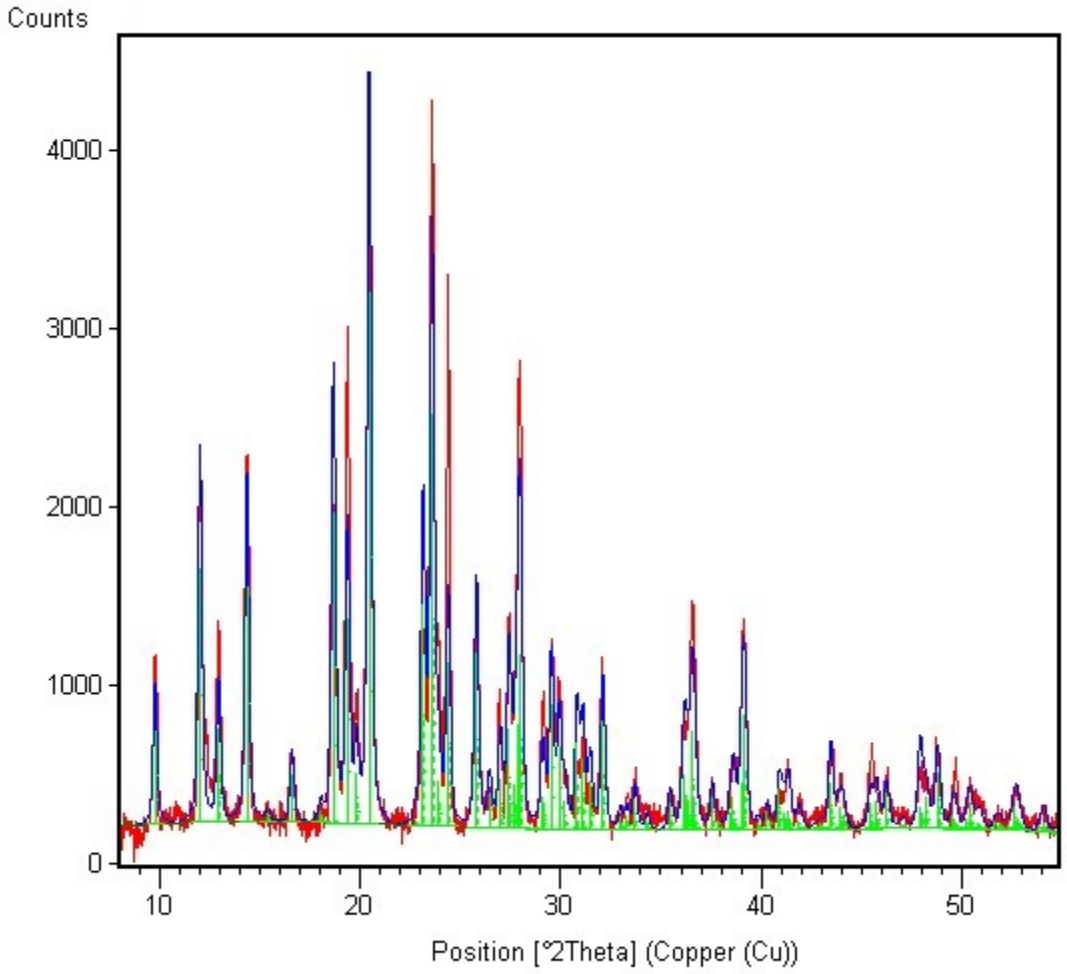

Figure S9. Observed and simulated X-ray powder pattern of *catena*-[Mn($\mu_{1,5}$-dca)$_2$(4-MOP-NO)$_2$] (**2**)

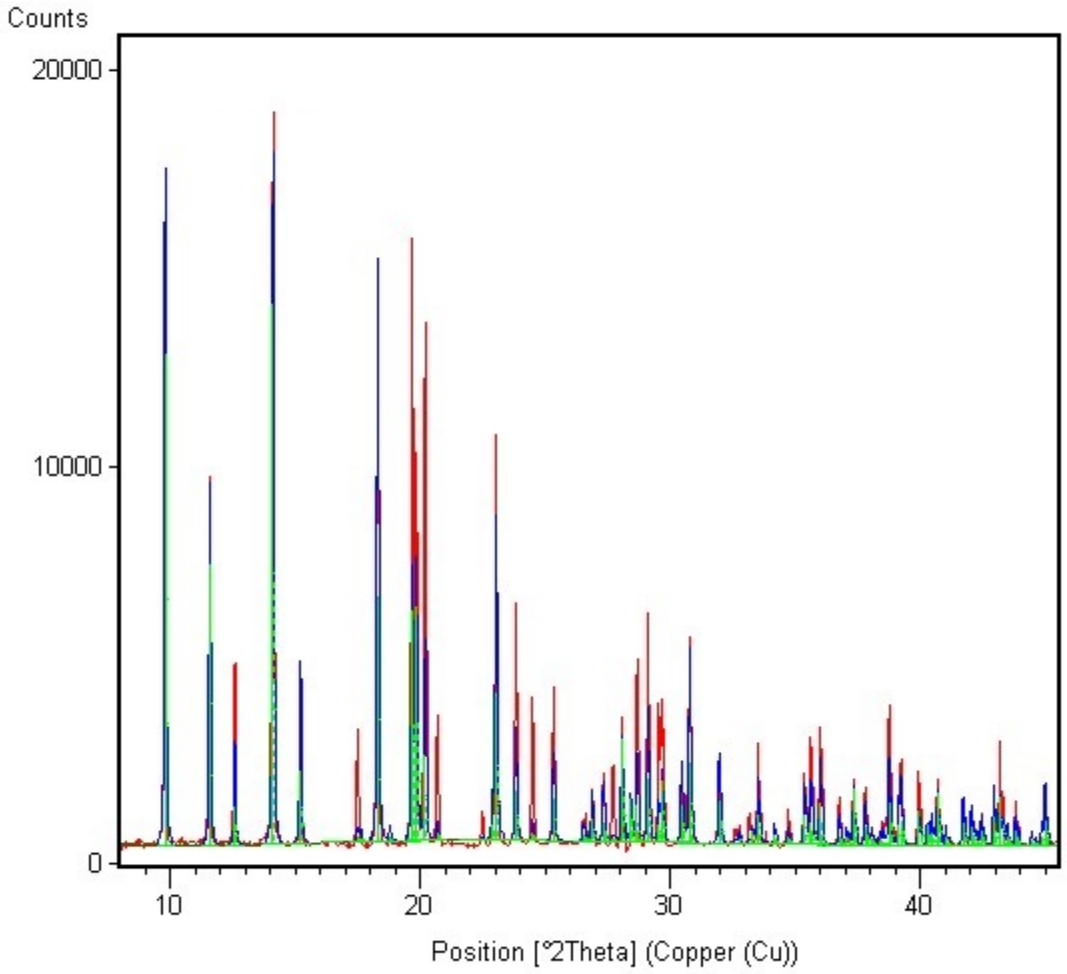

Figure S10. Observed and simulated X-ray powder pattern of *catena*-[Cd($\mu_{1,5}$-dca)$_2$(4-MOP-NO)$_2$] (**3**)

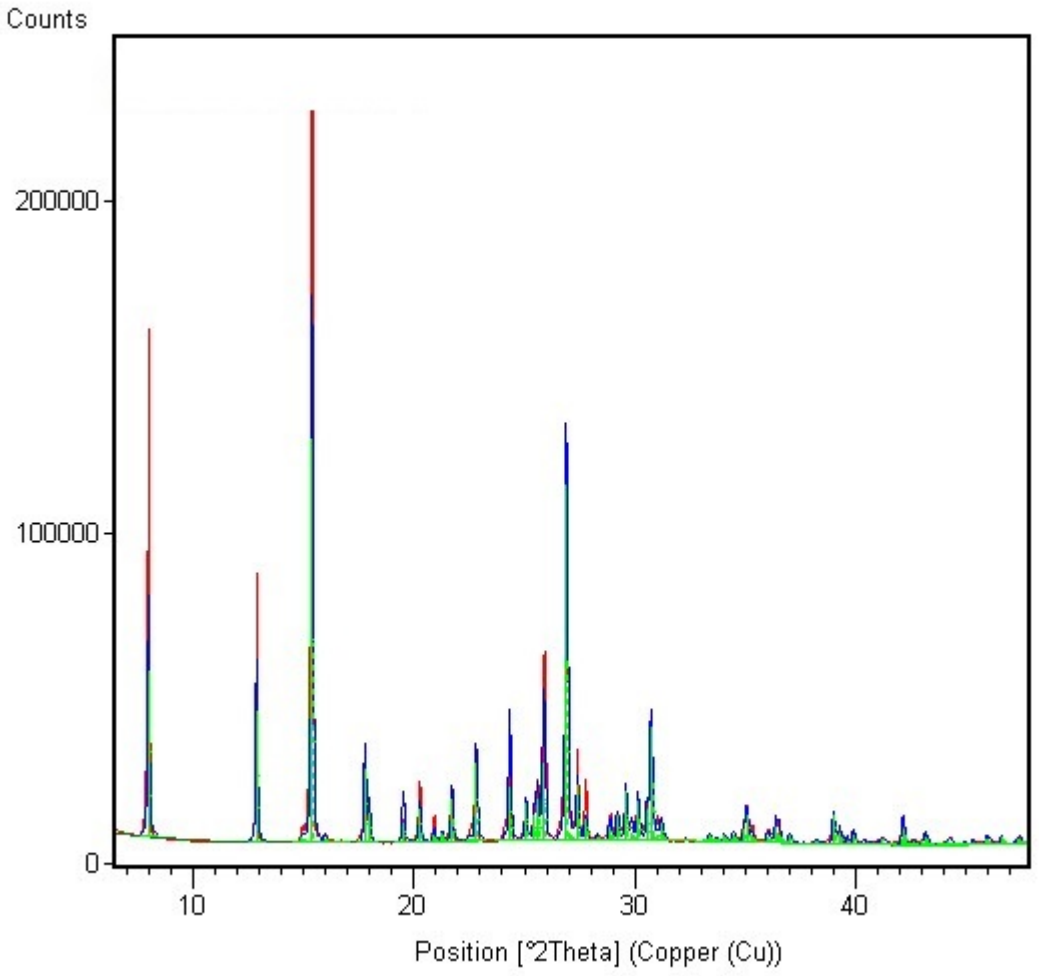

Figure S11. Observed and simulated X-ray powder pattern of $[Cu(\kappa^1\text{-dca})_2(4\text{-MOP-NO})_2]$ (**4**)